

Heat Transfer between Burned Gas and Cylinder-head in Rapid Compression Machines

R.Prawoto, T.Kageyama and F.Fisson

*Laboratoire d'Energétique et de Détonique
(URA 193 CNRS)*

E.N.S.M.A.

*Site du Futuroscope, 86960
France*

ABSTRACT

Pressure effects on the heat transfer between laminar flame and closed combustion chamber wall are studied by using a spark ignited rapid compression machine. Heat flux history on the internal face of the chamber is deduced from the local thermograms sampled on the external face of a measurement disc, by solving with nodal method, an one-dimensional non-steady inverse conduction problem. Good agreement between our results and that found in literature validates this method, which is well adapted to heat flux determination in dynamic systems.

It is found that, the non dimensional maximum heat flux $\Phi_{\max} = q_{\max}/q_c$ (q_{\max} : maximum value of unsteady heat flux from flames to combustion chamber wall, q_c : heat flux release rate by combustion prior to quenching) in one point:

a) decreases with pressure rise, proportionally to $P^{-0.8}$, b) is independent of equivalence ratio for a given pressure. A self-similarity law is observed on the evolution of Φ in function of a non dimensional time.

INTRODUCTION

Heat transfer, between gases and combustion chamber walls, is one of the important factors which determine the performance of internal combustion engines. Quite an amount of efforts have been done to elucidate the mechanism of such unsteady phenomena and to enable their prediction by numerical simulation technique.

On one hand, Grief et al. have shown experimentally and numerically that, during head-on¹ and sweeping² flame quenchings, the maximum value of unsteady heat flux q_{\max} from laminar premixed flames to combustion chamber wall, can be normalized by the heat flux release rate (flame power) prior to quenching q_c . For $P \approx 1$ bar and $T_w \approx 300$ K (T_w : wall temperature), they have shown, independently to the equivalence ratio and the fuel nature³, $\Phi_{\max} = q_{\max}/q_c \approx 0.3 - 0.4$ satisfies experimental data. On the contrary, they found Φ_{\max} depends on the wall temperature⁴. Their thermal flow sensor was a surface temperature type, consisting of a ceramic base coated with a thin film of platinum.

On the other hand, by using direct numerical simulations, Poinot et al.⁵ have found that: in the case of turbulent

premixed flame, the maximum value of non dimensional local heat flux corresponds, within 10 %, to the laminar heat flux (Fig. 1).

The purposes of our current experimental work, performed with two rapid compression machines, are to investigate, for laminar flames, the pressure effects on the heat transfer, by using the same normalizing parameter as Grief et al. and to verify the Poinot et al's proposition for turbulent flames. In this paper, we present some results on the first subject.

EXPERIMENTAL SYSTEM

The experimental set-up consisted of, two spark ignited rapid compression machines, an ignitor, heat flux and pressure measurement systems, a rapid shadow or schlieren image recording device and a mixture preparation unit. Details of these two machines have been presented in COMODIA 90 6,7

Combustion Chamber

The first machine⁶ (Fig. 2), used to study pressure effects, is equipped with a 60 mm bore flat head piston and a flat cylinder head parallel to the piston head. With a volume of 140 cm³ at B.D.C., a dead height of about 10 mm at T.D.C., a stroke of 50 mm, it has a B.D.C./T.D.C. volume ratio of about 6. A mirror piston and a Pyrex glass window are utilized for flame visualization. Spark electrodes cross the chamber along a diameter and, in this study, ignition has been performed at a point 6 mm apart from the cylinder wall and about 5 mm from the cylinder head. Due to the small value of the chamber height, the quenching in this machine is of the sweeping type, except in the vicinity of the ignition point where it is of the head-on one.

In this present study, the piston have been blocked at the end of compression, therefore constant volume combustion is realized.

Ignition has been performed by an inductance type spark generator currently utilized in car engines. The ignition timing has been regulated relative to the piston position by a delaying circuit. Propane-air mixture of different equivalence ratios has been prepared under a pressure of 15 bar in a bottle, by means of the partial pressure method. During each operation, piston position and pressure in the combustion chamber have been

recorded in function of time on a 12 bit numerical oscilloscope.

Rapid cinematography has been realized with a 60 mm wide drum camera. Light source was a 7 W Ar⁺ laser beam chopped by an acousto-optic external deviator. This configuration permits independent adjustments of image rate and of exposure time. For schlieren method, a circular stop has been used instead of classical knife edge.

Heat Flux Measurement

By solving with nodal method an one-dimensional non-steady inverse conduction problem⁸, heat flux history on the internal face of the chamber is deduced from the local thermograms sampled on the external face of a measurement disc (4 to 6 mm in diameter and 0.6 mm in thickness), made of the same duralmine as the cylinder head. This disc was fixed, with an isolating ring, at the bottom of one of the cavities, drilled into the thick cylinder head (Fig. 2-b). The thermograms (Fig. 3) are obtained by means of a I.R. sensor (Hg-Cd-Te) equipped by a silver halid (AgCl - AgBr) optical fibre ($4 < \lambda < 14 \mu\text{m}$) transmission system (Fig. 2-a). A preliminary calibration performed before each series of runs has led to an accuracy of about 0.1 °C.

Heat flux is then determined by a classical parameter estimation technique, which consists in optimizing, at each moment, in an iteratively way, the estimated heat flux and find the best fitting of temperature evolution with measured values. As observed on Fig. 4, obtained by using direct sighting (without optical fibre) and fine time resolution at the centre of a static pancake type chamber, heat flux shows several peaks during its history⁹. The first one, the duration of which is less than several hundreds of micro-second, corresponds to the heat exchange during flame quenching, investigated by Grief et al.. The second one, higher than the first, corresponds to the maximum of heat exchange between burned gas and wall. This second peak is what we interested in. The other peaks, which are lower than the two previous, appear after the end of flame propagation. Fig. 5 shows the good agreement between a measured thermogram and the retrieved thermogram obtained from the deduced heat flux history. It is worth to notice that, because of the geometry of sampling discs, our heat flow sensor is of integral type and adapted better to determine the second peak than the first one.

The use of the optical fibre, in spite of its lower signal level than that available by direct sighting method⁸ and of the loss of the resolution of the first peak, is motivated because it permits to eliminate the sight field loss due to the vibration of the machines^{10, 11}.

EXPERIMENTAL RESULTS

As described earlier, pressure effects has been examined during the propagation of laminar flames in the first machine. Thermogram sampling has been realized at seven locations (Fig. 2-c), respectively : N° 1 = -25 mm (Ignition point = - 24 mm), N° 2 = -20 mm, N° 3 = -10 mm (centre), N° 4 = 0 mm, N° 5 = 10 mm, N° 6 = 20 mm and N° 7 = 25 mm, located on the diameter issued from the ignition point. Investigations have been made with propane-air mixture of equivalence ratios ranging from 0.8 to 1.0. The chamber with the piston at T.D.C. is first drained out and then filled with compressed mixture, while the piston moves down to the B.D.C. The cylinder pressure is then adjusted to 1 bar and compression is

realized within 15 ms. The cylinder pressure increases to about 10 bar at the end of the compression, when ignition is performed. Then the pressure in the cylinder continues to increase because of the flame propagation. Simultaneous analysis of : flame position (Fig. 6), chamber pressure, ignition delay, timing of the visualization flashes (Fig. 7) and heat flux mapping at different positions on the cylinder-head (Fig. 8), allows to correlate these parameters.

Fig. 6 shows the general aspect of a 1.0 equivalence ratio propane-air mixture flames (exposure time 30 μs , interval 1.5 ms). After the spark energy is discharged, a flame kernel develops between the electrodes. 2.5 ms later, a spherical flame propagates along the longer electrode, while the flame front on the short electrode side is quenched near the cylinder wall. Two little outgrowths are observed on the upstream side of the flame surface. This local acceleration of the flame propagation is due to the turbulence created around the electrode during the compression phase. After its contact with the piston and cylinder heads ($t = 4.0 \text{ ms}$), the flame becomes cylindrical, and the increase of the outgrowths volume is still slow. From $t = 8.5 \text{ ms}$ to the end of the combustion, the volume of the protuberances expands rapidly and wrinkles are observed on the flame front. This is certainly due to the development of turbulence intensity generated by the interaction between the initial turbulence and the end gas movement triggered by the expansion of the burned gas. The propagation of the cylindrical flame front is somewhat slowed down by the reverse flow created by the rapid progression of the flame front in this zone. The general structure of this flame, however, remains laminar during the total duration of the flame propagation.

Heat flux evolutions at all sampling positions (Fig. 8) are the same, during the compression of unburned gas by the piston movement and the flame propagation, till they reached the plateau value, at the end of this phase ($q \approx 200 \text{ kW/m}^2$). Then it increases rapidly, because of the flame passage, to attain its maximum value and after that decreases with low frequency oscillations. The beginning of this second phase depends consequently on the sampling position. The maximum value during this phase increases with distance between the measuring and the ignition points ($2,7 \leq q_{\text{max}} \leq 3 \text{ MW / m}^2$). This trend is reasonable because the quenched gas temperature and pressure increase with the flame propagation. The heat flux values measured are in good agreement with that measured in engines¹².

The non dimensional maximum heat flux $\Phi_{\text{max}} = q_{\text{max}}/q_c$ is calculated by using the flame power $q_c = \rho_u S_u y_f (-\Delta H)$ with : ρ_u = unburned gas density, S_u = laminar burning velocity, y_f = mass fraction of fuel and ΔH = enthalpy of reaction. The instantaneous pressure P, for q_{max} of each sampling position, has been read from the pressure history recording, while the unburned gas temperature has been calculated by assuming an isentropic compression from the initial pressure (1 bar) to the current pressure P. The laminar flame velocity S_u has been calculated by using our data obtained by means of spherical chamber method¹³.

Table 1 gives the values of characteristic parameters for 7 sampling positions. For the point No. 2 to No. 6, while the pressure raises with flame propagation, q_{max} increases also. The points No. 1 and 7 are trivial because their positions are in the vicinity of the ignition point and the cylinder wall. If

normalized, Φ_{\max} decreases with pressure : $\Phi_{\max} \approx 0.25$ for $P \approx 10$ bar to $\Phi_{\max} \approx 0.15$ for 20 bar. These values are smaller than that obtained by Grief et al.¹ by means of a surface temperature type heat flux sensor, for $P \approx 1$ bar. Figure 9 shows the evolution of Φ_{\max} in function of the sampling position. In our pressure range, $\Phi_{\max} P^{0.8} = 1.5$ remains constant (Fig. 10). Dimensional analysis shows this pressure dependency is qualitatively in agreement with the relation : $hT^{0.52} / C_m \propto P^{0.8}$ (h = heat transfer coefficient, T = mean temperature of unburned and burned gas and C_m = mean piston speed) proposed for the heat transfer in engines¹⁴. The validity of this relation out of the studied conditions is not yet checked.

For a given pressure of about 12 bar, $\Phi_{\max} \approx 0.2$ is independent of equivalent ratio, which varies from 0.8 to 1 (Fig. 11). While the value of $\Phi_{\max} \approx 0.2$ is smaller than $\Phi_{\max} \approx 0.34$ found by Grief et al.³. for $P = 1$ bar, this result nevertheless confirms the effect of the equivalence ratio on Φ_{\max} they founded.

Fig. 12 shows a non-dimensionalized presentation of the heat flux history shown on Fig. 8. Here the time evolution of heat flux q , measured with a sampling disc, is normalized by q_{\max} corresponding to the same disc. The time t is normalized by a characteristic time t_q defined on Fig. 13. If $t/t_q = 0$ is adjusted for $q/q_{\max} = 1$, there is a good similitude between the heat flux histories.

CONCLUSION

Pressure effects on the heat exchange between propagating laminar flame and closed combustion chamber wall have been studied by using an ignited rapid compression machine.

1. The good agreement between our results and that found in literature validates this method, which is well adapted to heat flux determination in dynamic systems.

2. It is found that, the non dimensional maximum heat flux $\Phi_{\max} = q_{\max}/q_c$ in one point,

a) decreases with pressure rise, proportionally to $P^{-0.8}$,

b) is independent of equivalence ratio for a given pressure.

3. A self-similarity law is observed on the evolution of Φ in function of a nondimensional time t/t_q .

Heat exchange between turbulent flames and closed combustion chamber wall is now in progress.

We are also interested in the origin and physical meaning of the two peaks of heat flux observed during transient combustion.

REFERENCES

1. Vosen, S. R., Grief, R., and Westbrook, C. K., 20th Symposium (International) on Combustion. pp. 75-83, 1984.
2. Lu, J. H., Ezekoye, O., Grief, R. and Sawyer, R.F., 23rd Symposium (International) on Combustion. pp. 441-446, 1986.
3. Huang, W. M., Vosen, S. R., Grief, R., 21st Symposium (International) on Combustion. pp. 1853-1860, 1986.
4. Ezekoye, O., Grief, R. and Sawyer, R.F., Increased Surface Temperature Effects on Wall Heat Transfer During Unsteady Flame Quenching, 23rd Symposium (International) on Combustion. 1992.

5. Poinso, T. J. and Haworth D. C. : DNS and modeling of the interaction between turbulent premixed flame and walls, Center for Turbulence Research, Proceeding of the Summer Program 1992.
6. Kageyama, T. and Fisson, F., Proceedings of the 2nd International Symposium on Diagnostics and Modeling of Combustion in Internal Combustion Engines (COMODIA 90), J.S.M.E., pp 117-122, 1990.
7. Floch, A., Kageyama, T. and Pocheau, A., Proceedings of the 2nd International Symposium on Diagnostics and Modeling of Combustion in Internal Combustion Engines (COMODIA 90), J.S.M.E., pp 141-146, 1990.
8. Fort, C., Kageyama, T. and Saulnier, J. B., Identification of heat flux in the wall of a combustion chamber by solving an inverse conduction problem, Heat Transfer 1990 (Proceedings of IHTC 9, Jerusalem August 1990), August 1990, Hemisphere Publishing Corporation.
9. Fort, C., Estimation de paramètres et méthode inverse en thermique : Application à la détermination de la variation du flux pariétal dans une chambre de combustion, Ph. D Dissertation, E.N.S.M.A. - Université de Poitiers, septembre 1989.
10. Prawoto, Transfert de Chaleur entre les gaz et les parois de chambres de combustion de machines à compression rapide, Ph. D. dissertation, E.N.S.M.A. - Université de Poitiers, may 1993.
11. Prawoto, Kageyama, T. and Fisson, F., Heat transfer between burned gas and chamber wall in rapid compression machines, poster session, the 24th Symposium (International) on Combustion, July 1992, Sydney, Australia.
12. Gilaber, P. and Pinchon, P., S.A.E. Transactions Vol. 6, No. 880516, pp. 6839-6857, 1988.
13. Asnoun, A. Fisson, F., Kageyama, T., Maroteaux, D., Experimental determination of laminar burning velocity of hydrocarbon-air mixtures by means of a spherical combustion vessel, Concilium Amalfitanum Super Ignis Opera, Joint Meeting of the French and Italian Sections of the Combustion Institute June 1987, Amalfi, ITALY.
14. Woschni, G., S.A.E Technical Paper N0. 670931, pp. 3065-3083, 1967.

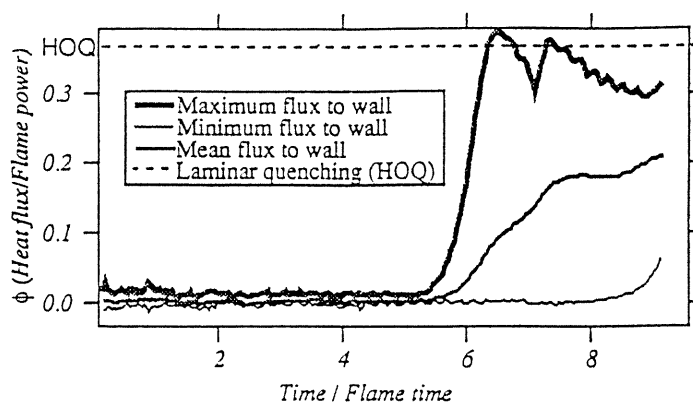
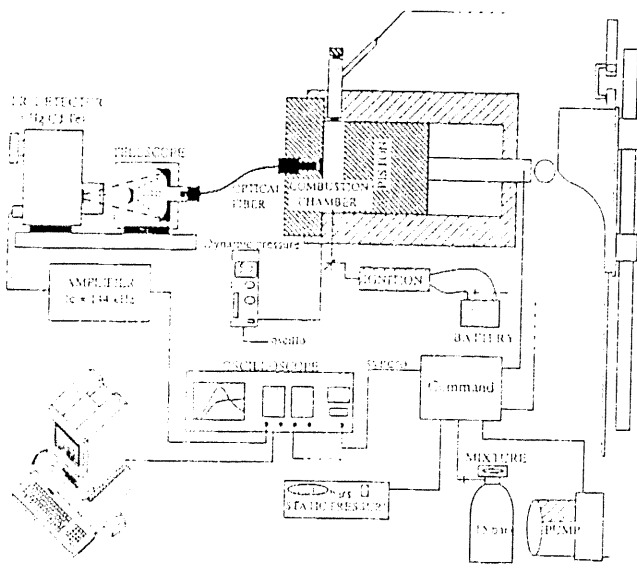
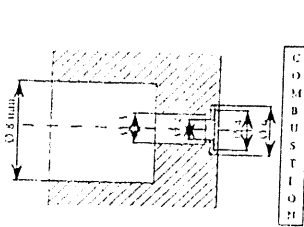


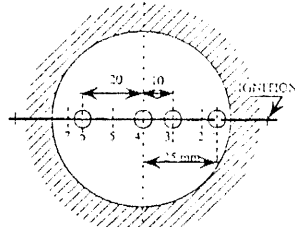
Fig. 1 : Maximum, mean and minimum heat flux exchanged between turbulent premixed flames and a wall (D.N.S. calculations)⁵



2-a: Schematic of the installation



2-b: Detail of heat flux measurement disc



2-c: Measuring positions

Fig. 2: Experimental setup

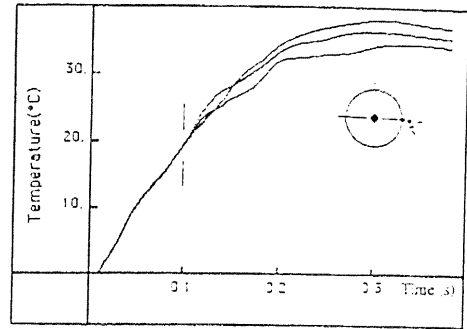


Fig. 3: Example of thermogram⁹

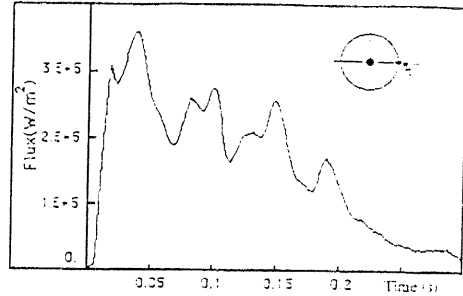


Fig. 4: Example of deduced heat flux⁹

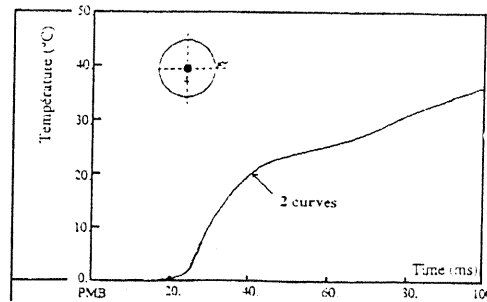


Fig. 5: Comparison between a measured thermogram and its retrieved thermogram¹⁰

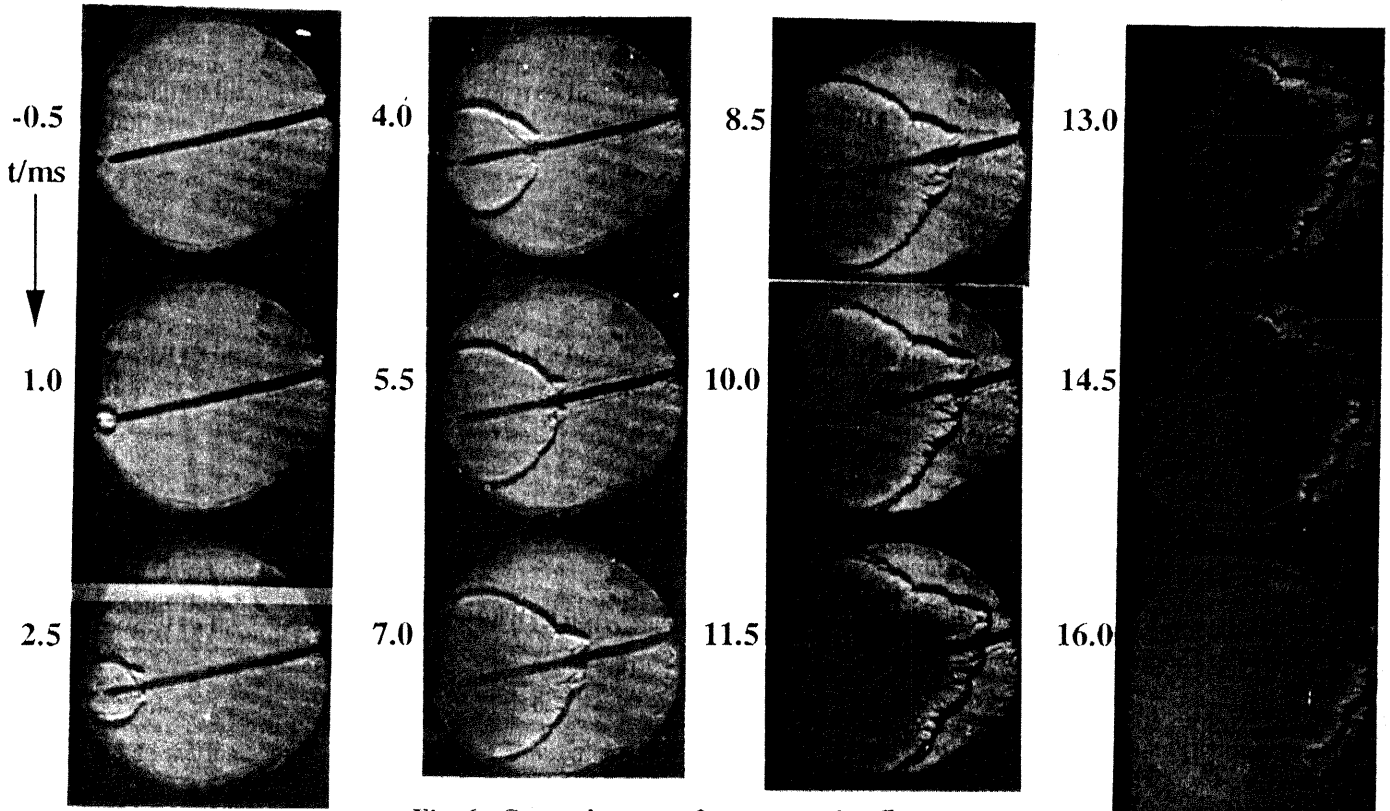


Fig. 6: General aspect of a propagating flame.
Equivalence ratio = 1; Time in ms.

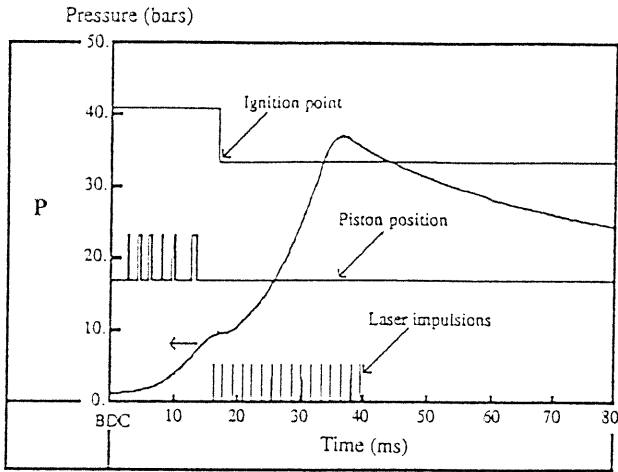


Fig. 7 : Pressure, piston position and laser flash recordings of the rapid compression machine

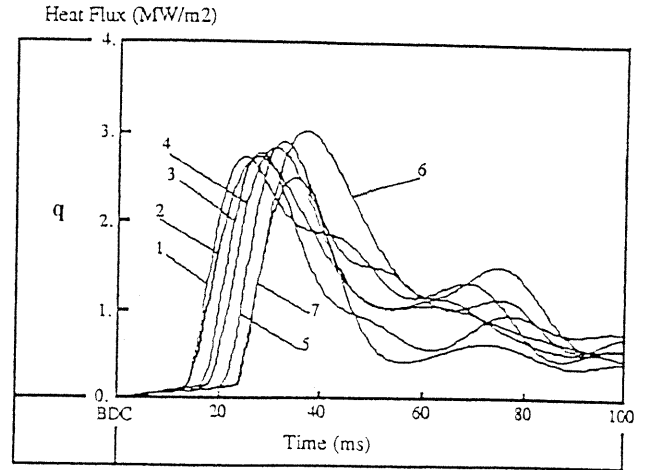


Fig. 8 : Heat flux mapping

Points	1	2	3	4	5	6	7
P (bar)	9,55	9,77	10,87	12,30	14,55	18,99	23,36
T (K)	471	474	487	504	526	565	597
Su (m/s)	0,52	0,52	0,54	0,55	0,57	0,61	0,63
ρu (kg/m ³)	7,52	7,64	8,27	9,05	10,24	12,46	14,51
q_{max} (MW/m ²)	2,74	2,61	2,71	2,83	2,91	3,03	2,50
q_c (MW/m ²)	10,82	10,99	12,35	13,76	16,14	21,02	25,28
Φ_{max}	0,25	0,24	0,22	0,21	0,18	0,14	0,10

Table 1 : Measured and deduced parameters at 7 measuring points

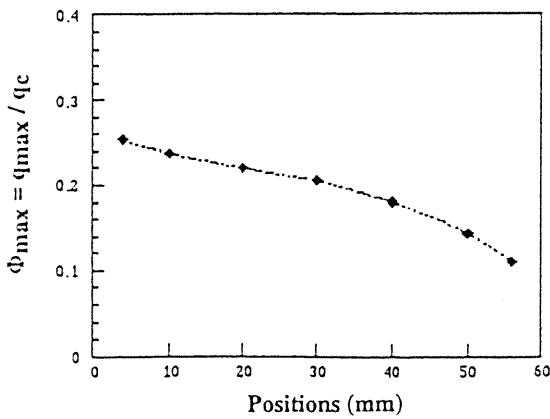


Fig. 9 : Φ_{max} along a diameter on the cylinder head (equivalence ratio = 1)

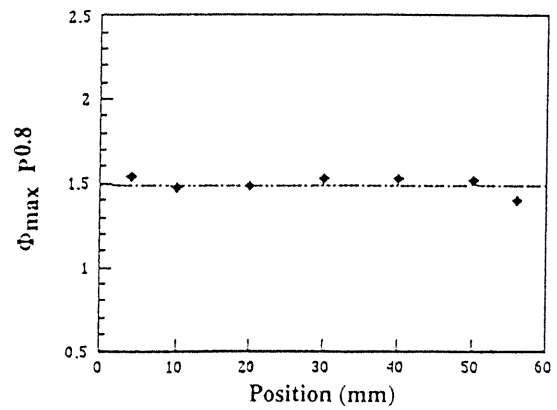


Fig. 10 : $\Phi_{max} P^{0.8}$ along a diameter on the cylinder-head

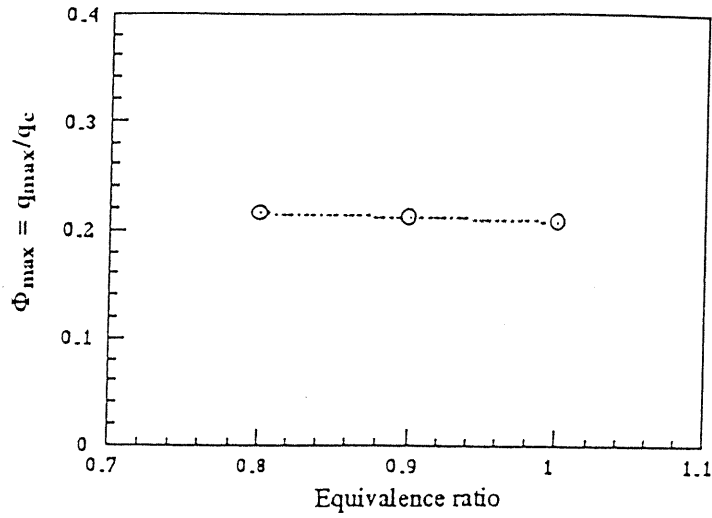


Fig. 11 : Φ_{\max} in function of equivalence ratio

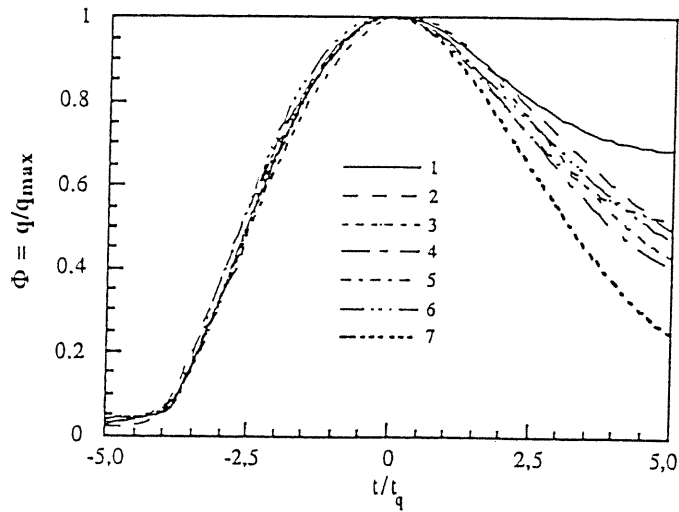


Fig. 12 Evolution of Φ in function of non-dimensional time t/t_q

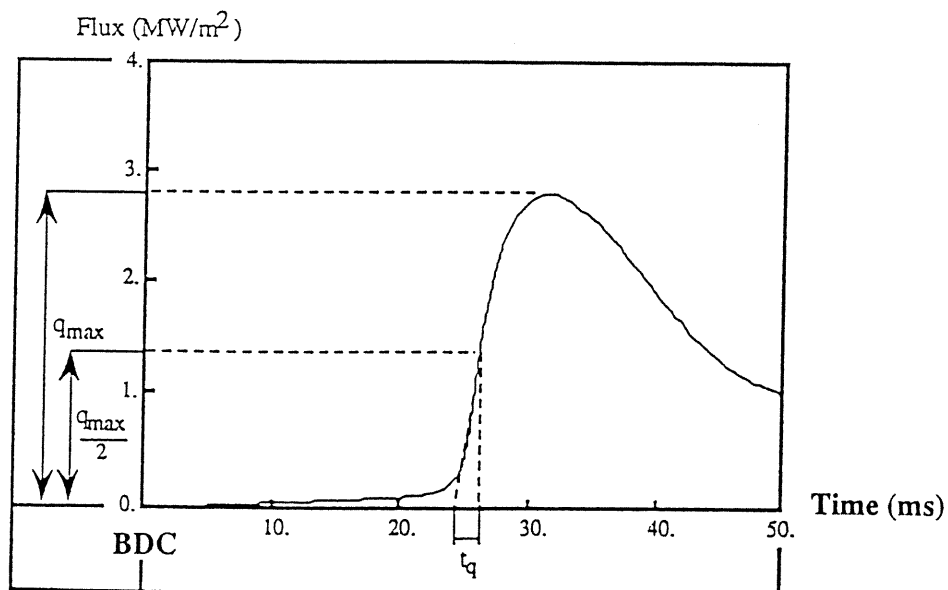


Fig. 13 : Definition of the characteristic time t_q